Oral Presentation

The 7th TSME International Conference on Mechanical Engineering
13-16 December 2016

TSME ICOME 2016
Mechanical Engineering Innovation for Green Society

AEC0009

Effect of Primary to Secondary Air Ratio on Combustion Performance for Pulverized Biomass Burner in Industrial Boiler

Narasad Phikun-ngoen[1], Jarruwat Charoensuk[1*], Monton Jhaikuson[1], Niwat Suksam[1], and Nuthvipa Jayranaiwachira[1]

[1] Department of Mechanical Engineering, Faculty of Engineering, King Mongkut's Institute of Technology Ladkrabang, Bangkok 10520, Thailand
[*] Corresponding Author: Tel.: +66 2 3298350; fax: +66 3298352; E-mail address: kcjarruw@kmitl.ac.th (J.Charoensuk)

Abstract

This research aims to investigate the factor of primary to secondary air ratio that influences the temperature in pre-chamber of 1 MW pulverized biomass burner. The air system in pulverized biomass burner is separated into three parts: primary, secondary and tertiary air. The experiment was performed as base case at the primary to secondary air ratio of 0.1538 and used for validation of the simulation. On simulation, swirl blades angle were fixed at 100 degrees, while the primary and secondary air flow rate were adjusted leading to the mass ratio variation. The comparison on each case was made on axial temperature. Among five cases of mass ratio (0.0714, 0.0769, 0.1250, 0.1333 and 0.1429), it was shown that the case for operation was found at the mass ratio of 0.1333. At this ratio, the maximum temperature and position were 1505.47 °C and 1.138 m, respectively, while the base case was 1415.05 °C and 1.404 m.

Keywords*:* Biomass Burner; Simulation; Primary Air; Secondary Air.

1. Introduction

In recent years, alternative energy has gained attention around the world because the energy demand is very high. The search for new alternative energy and using it with highest efficiency have received increasing attention. One of the interesting alternative energy resources is biomass. If utilized effectively, it will emit low pollution. Moreover, the main ingredients are bio organic substances including waste agriculture such as husk, sawdust and bagasse, etc.

Most combustion researches are based on empirical approach. It requires a huge experiment number, lot of cost, time and numerous resources compared with the numerical simulation for its low cost and high flexibility on application. The computational fluid dynamics (CFD) approach was used in this research to visualize the detailed of temperature distribution and flow field. Sharfi and Boroomand [1] validated the difference between the numerical and experimental data. The validation study showed that the maximum difference of the numerical and experimental results was up to 11%. Dong-Fang Zhao et al [2] optimized the geometrical parameters of the nozzle outlet to ejector inlet and nozzle outlet diameter of a premixed cylindrical burner for low pollutant emission by using CFD model. The result showed that the maximum discrepancy between the numerical and experimental results was about 3.1% at a=1.6. They explained that the reason for the discrepancies may originate from the assumption model, error from instruments system, experimental environment, approximate algorithm and operators, respectively. Thanaphat Phakdeeworrrawong [3] used the numerical model for coal combustion for simulation of pulverized biomass burner. He found the highly dispersed particle trajectories in a pre-chamber formed at 90 degrees of outlet wall angle. This could provide stable combustion without blow-off effect. Chinnapat Turakarn [4] studied the combustion characteristic of a pulverized biomass burner on a difference swirl blades angle. The results showed that at 100 degrees of swirl blades angle, the secondary air flow was able to induce recirculation within the pre-chamber, thus enabling the combustion stability. The pulverized biomass burner with pre-chamber can be operated at 300 kW to 500 kW which could be used for industrial applications.

The air flow rate has great influence on the temperature distribution, stability of flame and exhaust gas concentration formed by combustion process. Jianping Jing et al. [5] studied the influence of various primary air ratios with CFR swirl coal burner. He found that by decreasing the primary air ratio, the gas temperature, temperature gradient and carbon monoxide concentration in the nozzle region had increased, while nitrogen oxides decreased. Later, Jianping Jing et.al. [6] studied the influence of various mass flow rates (MFR) of secondary air on gas/particle flow characteristics of a CFR burner and found that at the MFR of 0.259 kg/s, large recirculation zone would occur. This resulted in stable combustion and also inhibited NOx formation.

In our pulverized biomass burner system, the unsuitability of the primary to secondary air ratio had caused a long flame and provided high temperature at

AEC0009

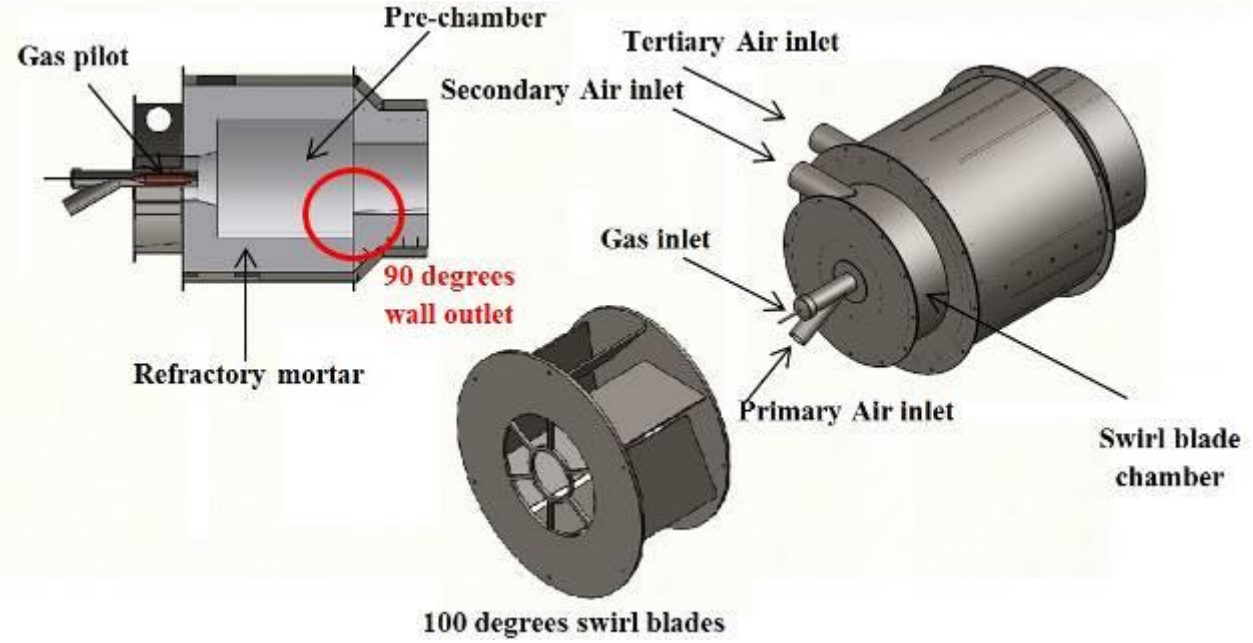

wet scrubber, which is a dangerous case. The study of air ratio is necessary. It has the advantages not only for

Fig. 1 Description of the pulverized biomass burner

safety of system but also the relevant person during operation.

In the present work, the investigation on the effect of primary to secondary air ratio will be presented aiming to reduce the length of flame and increase the temperature in the pre-chamber with 500 kW of pulverized biomass burner. Our approach is based on CFD prior to conducting experimental investigation in order to save time and resource.

2. Description of the pulverized biomass burner and system

Fig. 1 shows the pulverized biomass burner. It consists of the pre-chamber, refractory mortar, 100 degree swirl blades, gas inlet, gas pilot, biomass fuel-primary air mixture inlet, secondary air inlet and tertiary air inlet. The pre-chamber, starting from the gas pilot, is all covered by refractory mortar. The outer edge of refractory mortar has a tertiary air flow layer introduced for trapping heat of the flame. The refractory mortar is connected with 90-degree reduction component [3]. During operation, the pulverized biomass is transported by screw feeder and entrained by primary air through primary air inlet into a pre-chamber. At the same time, the secondary air from secondary air fan pass through 100 degrees swirl blades in swirl blade chamber, this swirl blade produces swirling air into the pre-chamber and generate recirculation within the pre-chamber. While burning, the tertiary air flowing through layer between refractory mortar and metal wall outside burner, passes through a tertiary port, creating cooling effect around the outer skin of the burner for safety of a person nearby. The pulverized biomass burner is designed at 1 MW. The recirculation in a pre-chamber has an important role on realizing combustion performance. There are two zones of recirculation in the chamber: i) internal recirculation zone (IRZ) and, ii) external recirculation zone (ERZ) see Fig.2b

(a) Photograph of pulverized biomass burner

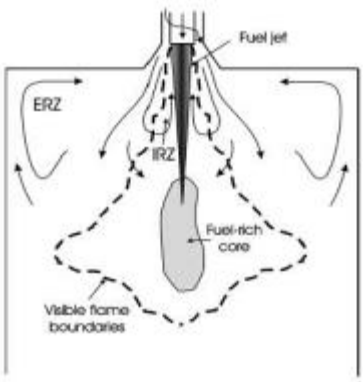

(b) Recirculation air in pre-chamber [7]

AEC0009

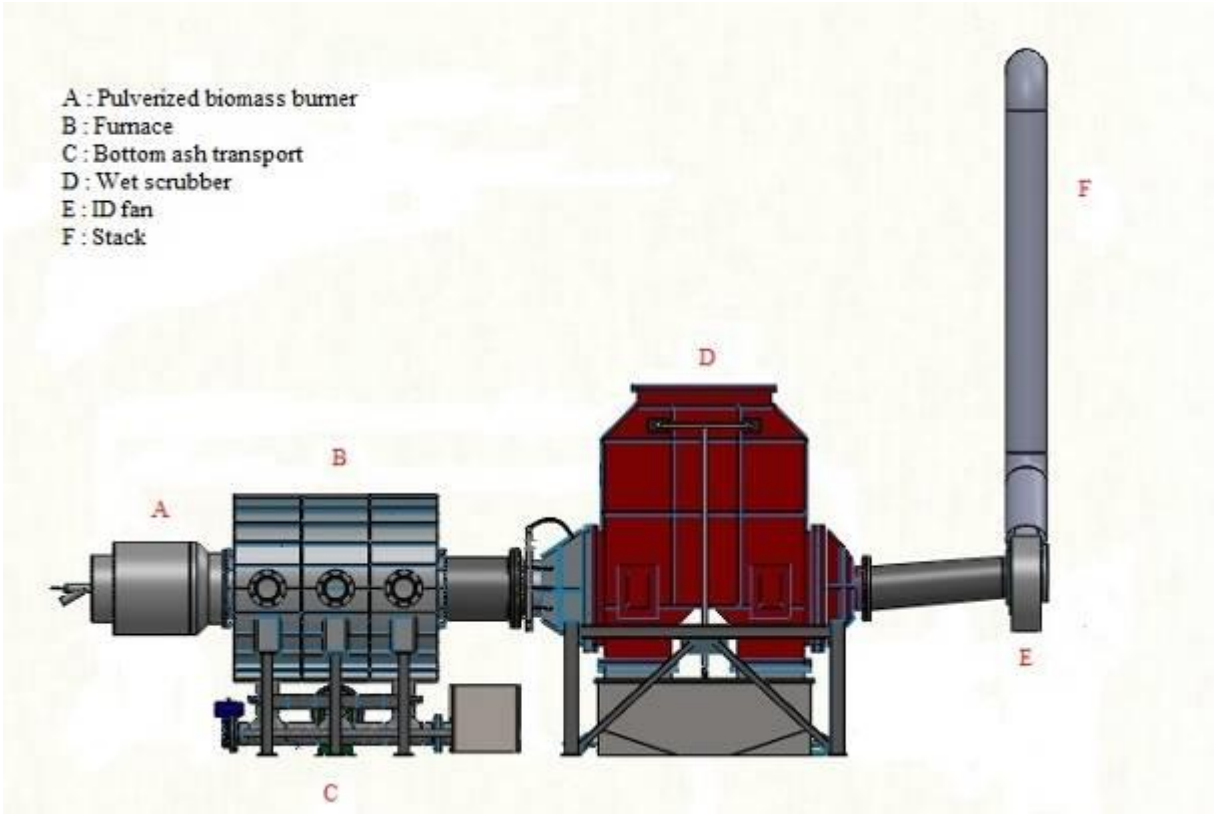

Fig. 2 The photograph of pulverized biomass burner
and recirculation air in pre-chamber
(a) Schematic diagram of experimental plant system

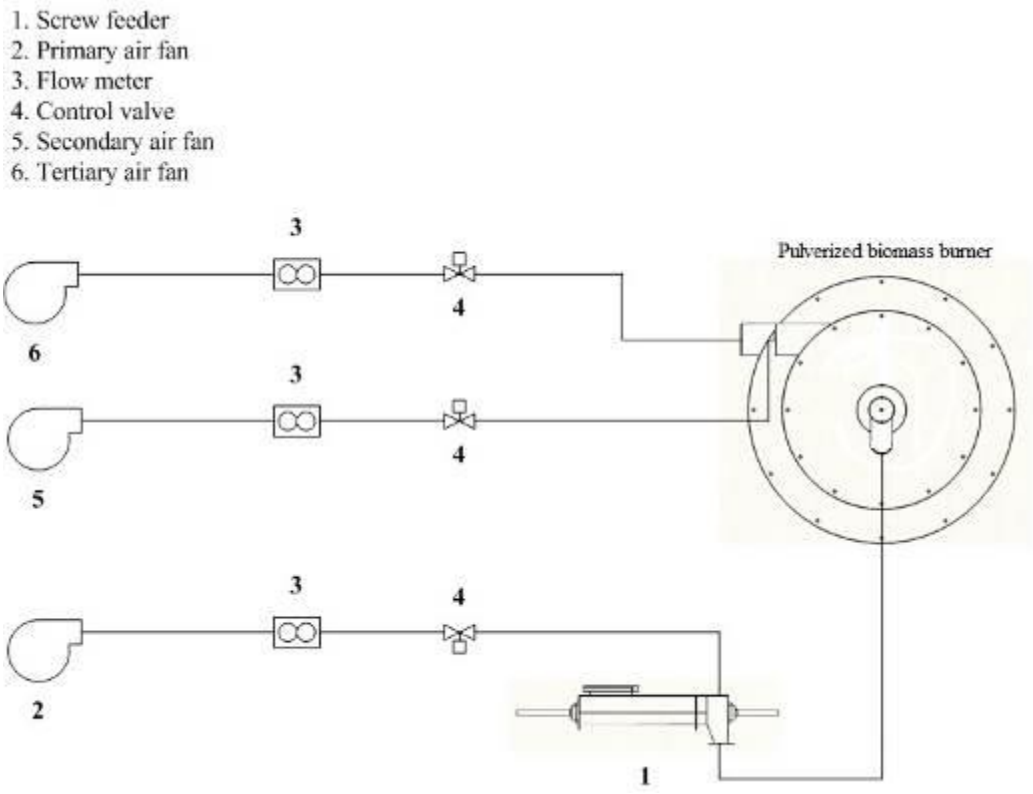

(b) Schematic diagram pulverized biomass burner of air system

Fig. 3 Schematic diagram of experimental plant and air system of pulverized biomass burner

For the gas pilot burner, it is intended for use to start the operation and warm up the system. The air system in pulverized biomass burner is separated into three parts: primary, secondary and tertiary air, as given in Fig.3b. The air flow of each part is driven by primary, secondary and tertiary air fan, respectively. The pulverized biomass is entrained by primary air flow at screw feeder outlet. Three proportional valves are controlled by ZXQ2004C positioner electric actuator [8] to adjust the air flow rates of the system. There are three orifice flow meters which have ISO 5167 connection with three kimo CP110 differential pressure transmitters with measuring range of ±100 Pa to ±2000 mbar [9] to measure the three flow rates of air inlet. Fig.3a shows a schematic diagram of the experimental plant. While combustion take place in a pre-chamber and furnace, locating under furnace is a bottom ash transport system. It has been installed to drain the bottom ash for continued operation of system. The ID fan plays an important role in drafting exhaust gas and fly ash from combustion process through a wet scrubber for cooling the exhaust gas and trap the fly ash by water spray inside the wet scrubber before passing through to the stack.

3. CFD model and boundary condition

This simulation work is based on 3D model. It takes long time to reach convergence. Therefore, the assumptions are made before calculation, the problem is assumed to be at steady state.

3.1 Gas phase modeling [10]

The gas phase flow is described by set the Reynolds-averaged Navier-Stocks equations to steady state, closed by the *k-ε* Standard turbulence model. The governing equations can be written as.

$$\nabla \cdot (\rho U \emptyset) - T_{eff} \nabla \emptyset = S_{\emptyset} \qquad (1)$$

Where U is mean velocity. ρ is density. $S_{\emptyset}$ is source term. The governing equations solved for gas phase include various parameters which summarized in Table 1.

3.2 Particle phase modeling [11]

The Lagrangian method was adopted for the particulate phase suspending in the flow. The interaction between particulate and gaseous phases are related through the transfers of mass, momentum and energy. The source terms can be calculated by using Particle Source in Cell Techniques [12] shown in Fig.4

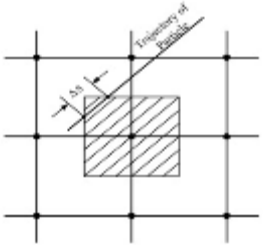

Fig. 4 Trajectory of particle for Lagrangian's Method

Table. 1 Variables $\emptyset$, T_{eff} and $S_{\emptyset}$ in governing equation for gas phase

	$\emptyset$	T_{eff}	$S_{\emptyset}$
Continuity	1	0	Total mass transfer rate from particle phase
Momentum	*u,v*	$\mu + \mu_1$	Drag forces of particle
Energy	*H*	$\lambda + \frac{\mu_1}{\sigma_H}$	Reaction heats and convection/radiation heat transfers from particle phase
Species mass fraction	Y_1	$\mathrm{T} + \frac{\mu_1}{\sigma_{Y_1}}$	Chemical reaction rate involving component *i*
Turbulent kinetic energy	*k*	$\mu + \frac{\mu_t}{\sigma_k}$	$P_k - \rho_z$
Turbulent dissipation rate	ε	$\mu + \frac{\mu_t}{\sigma_z}$	$C_1 \frac{\varepsilon}{k} P - C_2 \rho \frac{\varepsilon^2}{K}$

$$\mu_t = C_\mu \rho \frac{k^2}{\varepsilon}, P_k = (\mu + \mu_t)\nabla U \cdot (\nabla U + (\nabla U)^T)$$

$$C_\mu = 0.09, C_1 = 1.44, C_2 = 1.92$$

3.3 CFD model

The CFD solved by software ANSYS FLUENT 12.0 and used the species transport, *k-ε* Standard turbulence model by increasing 2.5 times the default parameter of the oxygen diffusion surface rate of char particle (C_1) and kinetic reaction rate of char particle (C_2) and used the random walk model for turbulent effect on particle trajectories. The kinetic parameters are shown in Table 2.

Table. 2 Kinetic parameters for biomass combustion

Kinetic parameters: Devolatilization, E (J/kg-mol) Pre-Exponential Factor	 7.40×10^7 3.82×10^5
Char reaction, E (J/kg-mol)	7.90×10^7

The wood pellet made from rubber tree was used in this work. The ultimate analysis has been characterized by Thailand Institute of Scientific and Technology Research (TISTR) [13] as given in Table 3. The comparison on primary to secondary air ratio case was made with respect to axial temperature distribution. This ratio is calculated by Eq. (2) and known that mass ratio. The various air boundary

conditions are simulated in order to compare for different operation cases shown in Table 4.

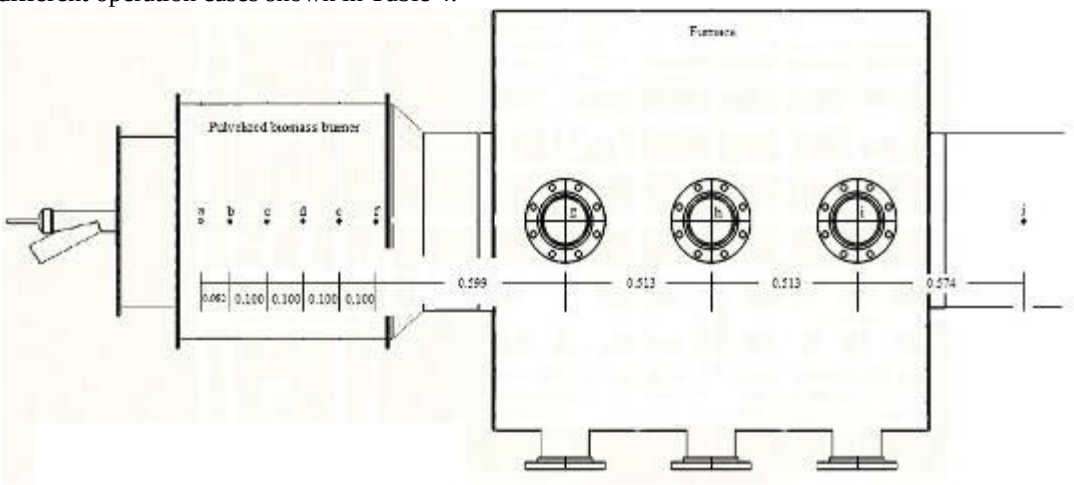

Fig. 5 The position description of pores for insertion thermocouples

Table. 3 Characteristics of rubber wood pellet [13]

Proximate analysis	(% mass)
Volatile	76.68
Fixed carbon	15.23
Moisture	5.81
Ultimate analysis	**(% mass)**
Carbon	45.42
Hydrogen	6.31
Nitrogen	0.45
Sulphur	0.00
Oxygen	45.54
GCV (MJ/kg)	17.50

$$\text{Mass ratio} = \frac{\dot{m}_{primary}}{\dot{m}_{secondary}} \qquad (2)$$

Where $\dot{m}_{primary}$ is the mass flow rate of primary air (kg/s) and $\dot{m}_{secondary}$ is the mass flow rate of secondary air (kg/s).

4. Results and discussions

In the experimental set up, the pulverized biomass burner and furnace were installed with thermocouples along axial distance for measurement of temperature. As mentioned above, special attention was made on temperature in a pre-chamber. Therefore 5 locations of temperature are monitored in a pre-chamber. The position description and point detail of monitoring locations are shown in Fig.5 and Table 5, respectively.

Table. 4 Air boundary conditions for simulation

Case	Air mass flow rate						Mass ratio
	Primary		Secondary		Tertiary		
	kg/s	%	kg/s	%	kg/s	%	
Base	0.0223	10	0.1449	65	0.0557	25	0.1538
1	0.0111	5	0.1560	70	0.0557	25	0.0714
2	0.0111	5	0.1449	65	0.0668	30	0.0769
3	0.0223	10	0.1783	80	0.0284	10	0.1250
4	0.0223	10	0.1671	75	0.0334	15	0.1333
5	0.0223	10	0.1560	70	0.0446	20	0.1429
Total air mass flow rate 0.2229 kg/s					Fuel mass flow rate 0.0317 kg/s		

Table. 5 Point details of pores in Fig.5

Position	*Description*
a	Outlet of biomass fuel-primary air mixture pipe
b	Pre-chamber 1
c	Pre-chamber 2
d	Pre-chamber 3
e	Pre-chamber 4
f	Pre-chamber 5
g	Furnace 1
h	Furnace 2

i	Furnace 3
j	Flue gas

4.1 Validation for combustion simulation results

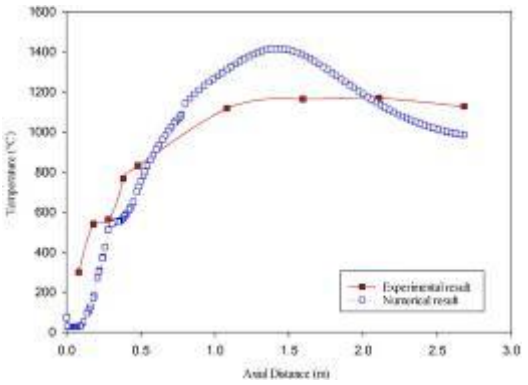

Fig. 6 Comparisons between combustion simulation results of base case temperature and experimental data

The experiment was performed as base case at the mass ratio of 0.1538 and used for validation. Fig.6 shows the simulation results of the base case temperature as compared with the experimental data. The maximum difference between simulation results and experimental results is about 19.33% at axial distance =1.594 m. the difference is observable in the pre-chamber and in the furnace. Similar to the study found in existing literature [2] the reason of the difference between the simulation and experimental results may originate from the assumptions of models being used, simplifications of the problem, error from instruments system, experimental environment, approximate algorithm and operators, respectively.

4.2 Simulation results of base case along the axial symmetry cross-section

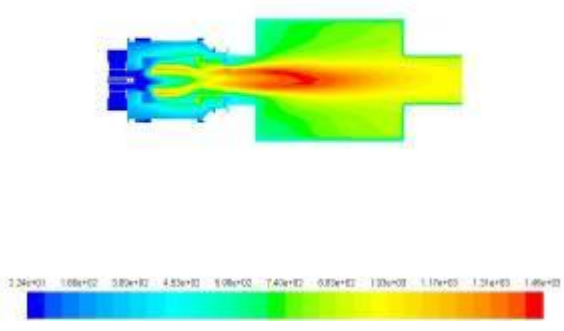

Fig. 7 Base case temperature distributions along the axial symmetry cross-section

Fig.7 shows the temperature distributions along the axial symmetry cross-section. It depicts the flame length of base case. It is noticeable that temperature at furnace outlet zone is high because the turbulence and residence time of fuel in pre-chamber is too low and pulverized biomass fell out abruptly from mixing during combustion process. This can be observed in Fig.8

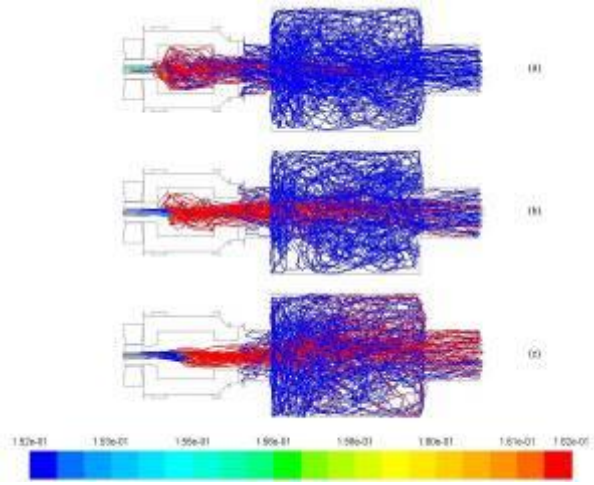

Fig. 8 Mass fraction of char particle trajectory (base case); (a) 37.50-112.5, (b) 165.0-240.0, (c) 362.5-500.0 µm

Fig.8 shows the mass fraction of char particle along with its trajectory for the base case. It consists of three diameter ranges i.e.; 37.50-112.5, 165.0-240.0, and 362.5-500.0 µm. Most of char particles are found well-dispersed in the pre-chamber, especially for the diameter range below 112.5 µm which is also found in ERZ. This is because small char particle has low momentum than large char particle. The momentum of large char particle can overcome the momentum of air recirculation in the pre-chamber and start to dispersed further away from the burner exit plane. This is not so when considering the momentum of small char particle. From the issue aforementioned, the decrease in temperature at furnace outlet and the decrease in flame length are achieved by increasing the turbulence in pre-chamber, especially for the cases with char residence time being longer than the base case. This can be described by case 1 through to case 5 in the next topics.

4.3 Simulation results of case 1 and case 2 along the axial symmetry cross-section

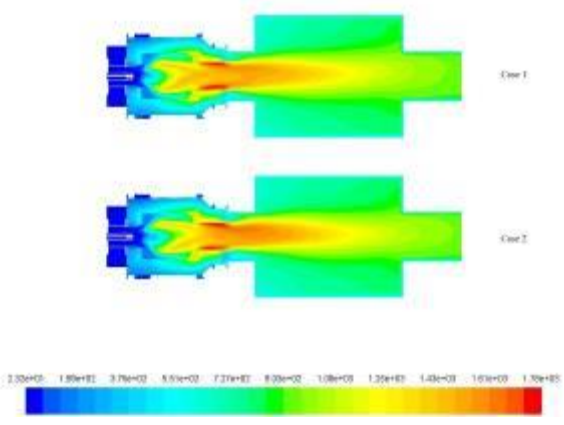

AEC0009

Fig. 9 Temperature distributions of case 1 and case 2 along the axial symmetry cross-section

Fig. 9 shows the temperature distributions of case 1 and case 2 along the axial symmetry cross-section, where the mass ratio is 0.0714 and 0.0769, respectively. The effect of mass ratio among case 1 and case 2 are small because the difference in mass flow ratio is around 5 %, referring to the numerator in Eq. (2). When decreasing the mass ratio further, it is noticeable that the process could continue to achieve stable combustion but there are hotspots at outlet wall of the burner.

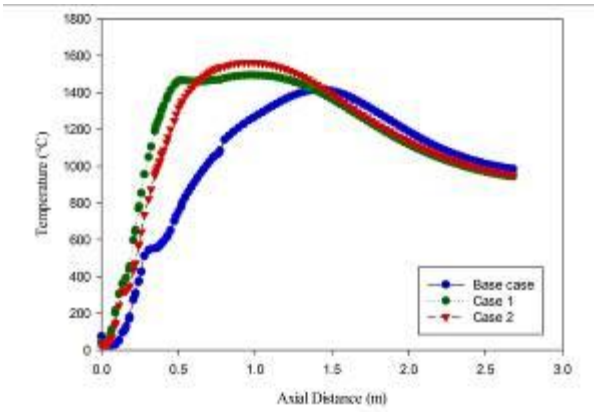

Fig. 10 Axial temperature of base case, case 1 and case 2

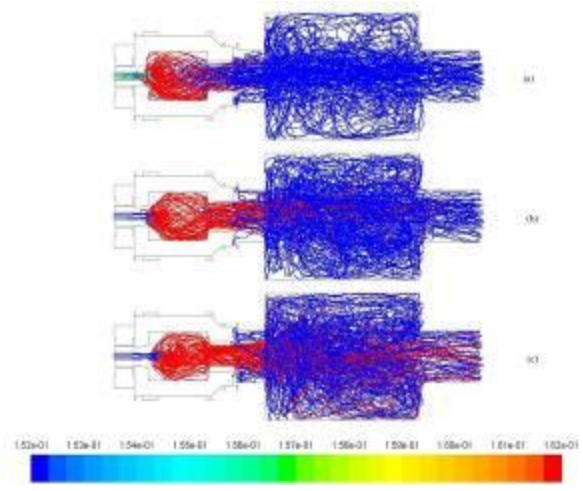

Fig. 11 Mass fraction of char particle trajectory (case 1); (a) 37.50-112.5, (b) 165.0-240.0, (c) 362.5-500.0 µm

Fig. 10 depicts the variation of the axial temperature with the decrease in mass ratio. The axial temperature of case 1 and case 2 are very similar. In both cases, dispersion of char particle significantly increases with decreasing in mass ratio because the momentum of all particle size decrease (observation in Fig.11 – 12). This results in an increase in temperature of a pre-chamber. High temperature is observed at the throat between pre-chamber and the main furnace. This hotspot shall be avoided in real situation in order to prevent thermal damage of the system.

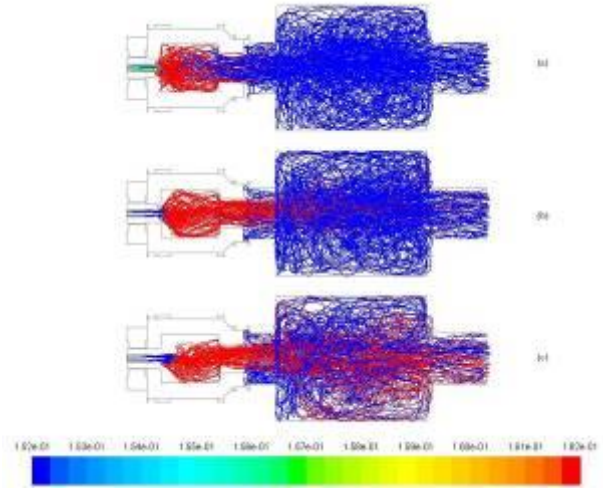

Fig. 12 Mass fraction of char particle trajectory (case 2); (a) 37.50-112.5, (b) 165.0-240.0, (c) 362.5-500.0 µm

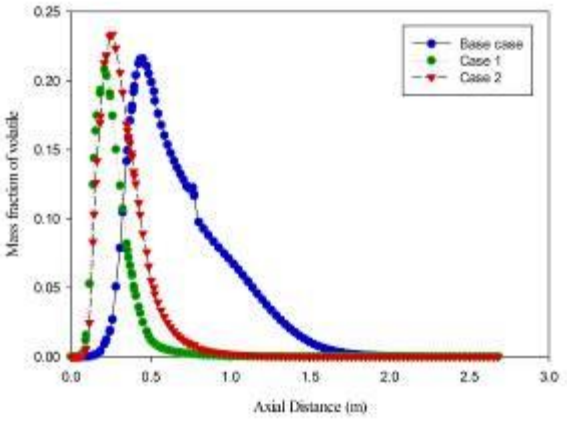

Fig. 13 Axial mass fraction of volatile of base case, case 1 and case 2

AEC0009

Fig. 13 shows the mass fraction of volatile along axial distance, which consistent with axial temperature and mass fraction of char particle. For base case, there is a relatively low concentration in a pre-chamber, therefore an intense volatile burn out take pace outside the pre-chamber next to the tertiary air inlet. For case 1 and case 2, however, Peak value of volatile concentration is well within the pre-chamber region and sharply decrease by an intense combustion taking place at the throat of the pre-chamber. Case 1 is performed by increasing the secondary air mass flow rate, which can induce the internal recirculation well within the pre-chamber, while case 2 has a slightly difference in mass ratio compared to case 1. It creates slight delay in volatile falling pattern as a result of delayed volatile combustion along axial distance as compared to case 1.

4.4 Simulation results of case 3, case 4 and case 5 along the axial symmetry cross-section

Fig. 14 shows the temperature distributions of case 3 case 4 and case 5 along the axial symmetry cross-section, with the mass ratio of 0.1250, 0.1333

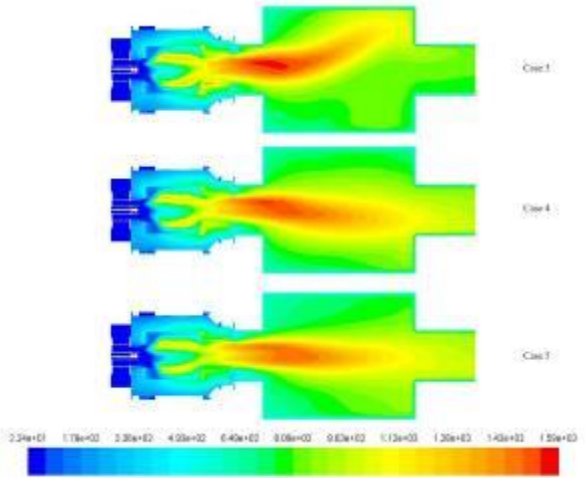

Fig. 14 Temperature distributions of case 3, case 4 and case 5 along the axial symmetry cross-section

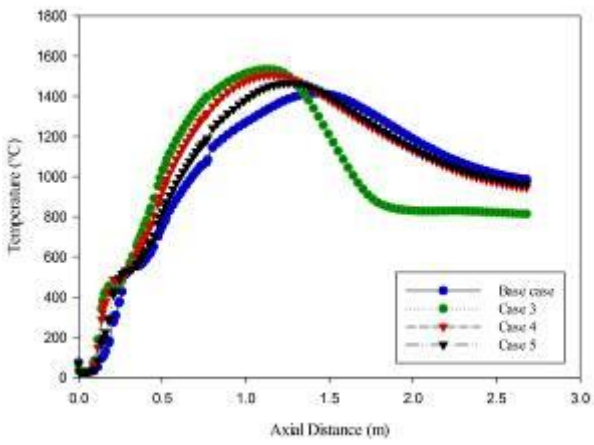

Fig. 15 Axial temperature of case 3, case 4 and case 5

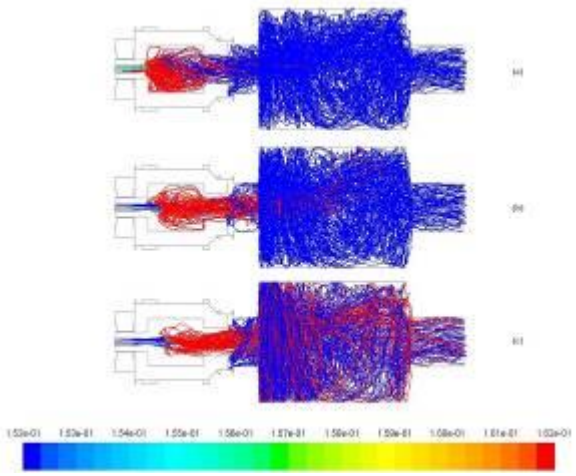

Fig. 16 Mass fraction of char particle trajectory (case 3); (a) 37.50-112.5, (b) 165.0-240.0, (c) 362.5-500.0 µm

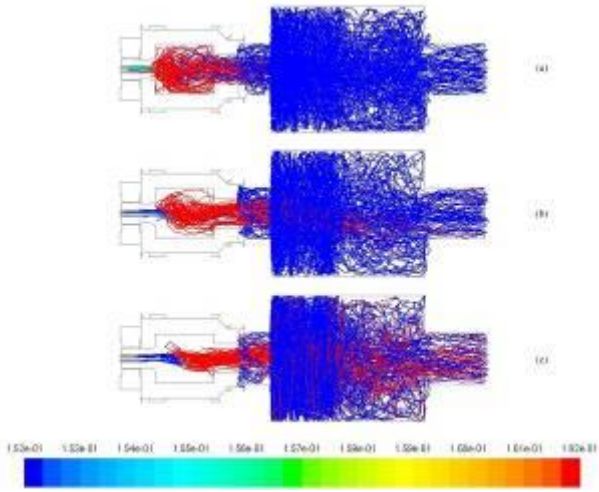

Fig. 17 Mass fraction of char particle trajectory (case 4); (a) 37.50-112.5, (b) 165.0-240.0, (c) 362.5-500.0 µm

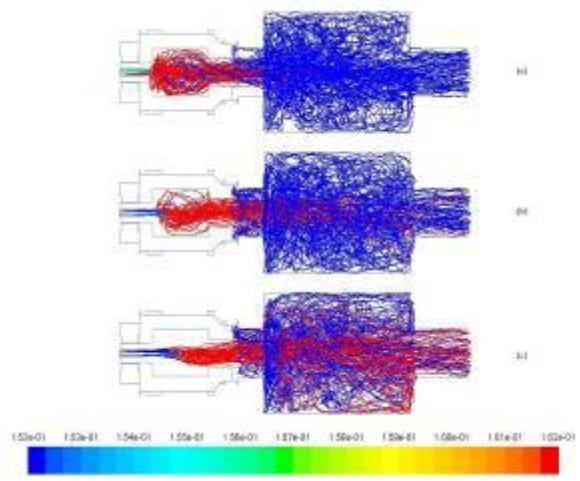

Fig. 18 Mass fraction of char particle trajectory (case 5); (a) 37.50-112.5, (b) 165.0-240.0, (c) 362.5-500.0 µm

and 0.1429, respectively. The increment of secondary air mass flow rate (by 5%) has caused slightly decreased in the mass ratio. This is because the mass flow rate of secondary air is the denominator, see Eq. (2). At the mass ratio of 0.1429, it is noticeable that it stable could be achieved but when the mass ratio is 0.1333 the flame begin to flick and severely flick when the mass ratio is 0.1250. This suggest that tertiary air has a strong influence on the flame shape in the furnace. The effect of buoyancy force for case 3 is most severe while in case 4 is lower and become insignificant in case 5.

Fig. 15 shows the axial temperature of the base case compared with case 3, case 4 and case 5. The result indicates that there are some differences among them. In case 3, at a distance about 1.4 m from the primary exit port, the temperature is highest. This is due to effect of large reverse flow and high turbulence in the pre-chamber created by angular momentum of the secondary air. Severe flick in flame shape is evidenced by relatively higher axial temperature compared with cases 4 and 5.

As far as burnout of char particle is concerned, the amount of left-over mass fraction of char for all cases are presented in Figs 16, 17 and 18. Although the particle trajectories are quite different, it was found that the effect of secondary to tertiary air ratio on degree of char burner out is not significant.

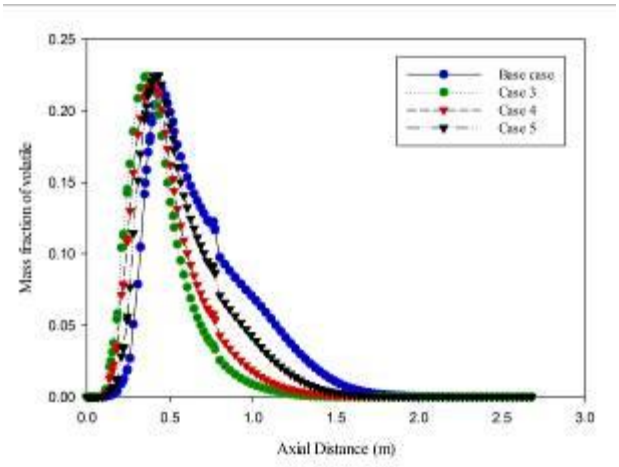

Fig. 19 Axial mass fraction of volatile of base case, case 3, case 4 and case 5

Fig.19 indicated clearly that devolatilization of case 3, 4 and 5 occur earlier than the base case. This corresponds to the amount of secondary air which directly relate to an angular momentum in the pre-chamber. Due to highest reverse flow in pre-chamber, the combustion volatile of case 3 can be completed before other case. This is consistent with those described earlier that this case has the highest axial temperature at axial distance at about 1.4 m.

It should be noted that the more turbulence taking place in pre-chamber, the earlier devolatilization occur. It creates high temperature in a pre-chamber and reduces the length of flame in operation. From the simulation results, it was shown that the case for highest temperature in pre-chamber was found at the mass ratio of 0.1250 but this mass ratio could not provide desirable flame shape due to influence of buoyancy force. Therefore, the mass ratio of 0.1333 was considered for operation case as there is a little flick of flame which is acceptable, while reduction of flame length could be achieved. Moreover, it satisfy safety requirement as hotspot at the connecting rod can be avoided although the temperature in a pre-chamber was higher than the base case and case 5. Therefore, this case has enough features to be appointed as operation case for our 1 MW pulverized biomass burner.

5. Conclusions

Simulation study is carried out to investigate temperature distribution, the trajectory of char particle and devolatilization on five cases of different mass ratios among primary secondary and tertiary air at 500 kW firing rate. Comparison is carried out with the base case in terms of the stability of flame, safety, and flame length. The following conclusions are made:

(1) Chaotic movements of char particles and reverse flow in a pre-chamber are closely related to devolatilization rate.

(2) The primary air mass flow rate has a great influence on aerodynamics in the combustion chamber. At low primary air corresponding to the primary/secondary mass ratio of 0.0714 and 0.0769, the condition could provide increased temperature in a pre-chamber, but the flame is large and create hotspot on surface of the refractory, bringing about safety issue in furnace operation.

(3) At relatively higher primary air flow rate together with the primary/secondary mass ratio of 0.1250 the burner provides increased temperature in a pre-chamber than other cases. It gives high char particle turbulence because of a large swirl effect of secondary mass flow rate, causing severely flick of the flame shape. The peak temperature is maximum among other cases.

(4) By keeping the primary air as the base case while keeping the primary/secondary mass ratio of 0.1333, desirable operating condition was achieved, as it could provide increased temperature in a pre-chamber without severe flicking of the flame shape and the axial distance of maximum temperature would shift to 1.138 m. The maximum temperature was 1505.47 °C, while the base case was at 1.404 m and 1415.05 °C, respectively.

6. Acknowledgement

The authors would like to thanks center for data storage technology, KMITL, for providing the computing resources and access of software used in this research work.

7. References

[1] Sharfi and Boroomand M. An investigation of thermo-compressor design by analysis and experiment: Part1. Validation of the numerical method, *Energy Conversion and Management*, vol.69, January 2013, pp. 217-227.

[2] Dong-Fang Z., Feng-Guo L., Xue-Yi Y., Rui Z., Bin-Long Z. and Gui-Long H. Optimization of a premixed cylindrical burner for low pollutant emission, *Energy Conversion and Management*, vol.99, April 2015, pp. 151-160.

[3] Thanaphat Phakdeeworrrawong. Mathematical simulation for pulverized fuel combustion, Thesis of King Mongkut's Institute of Technology Ladkrabang, 2013.

[4] Chinnapat Turakarn. Biomass burner development in industrial boilers, Thesis of King Mongkut's Institute of Technology Ladkrabang, 2015.

[5] Jianping J., Zhengqi L., Qunyi Z., Zhichao C. and Feng R. Influence of primary air ratio on flow and combustion characteristics and NOx emissions of a new swirl coal, *Energy*, vol.36, December 2010, pp. 1206-1213.

[6] Jianping J., Zhengqi L., Lin Wang, Lizhe C. and Guohua Y. Influence of secondary air mass flow rates on gas/particle flow characteristics near the swirl burner region, *Energy*, vol.36, March 2011, pp. 3599-3605.

[7] J.Ballester, J.Barroso, L.M. Cerecedo and R. Ichaso. Comparative study of semi-industrial-scale flames of pulverized coals and biomass, *Combustion and Flame*, vol.141, February 2005, pp. 204–215.

[8] JP Communications Inc., USA., URL: http://www.manufacturer.com/zxq2004c-electric-valve-positioner-servo-controller-actuator-products-p6983265

[9] PJ Bonner, Calibration Services Company, Ireland., URL:http://www.pjbonner.com/wp-content/uploads/Kimo-Sensors-Brochure.pdf Pressure sensor kimo CP110

[10] Y.S. Shen, B.Y. Guo, A.B. Yu and P. Zulli. A three-dimensional numerical study of the combustion of coal blends in blast furnace, *Fuel*, vol.88, September 2008, pp. 255–263.

[11] J.Charoensuk. The application of mathematical model for scaling pulverized coal combustors, Ph.D Thesis, University of London, 1996

[12] S.M.A. Rizvi. Prediction of flow combustion and heat transfer in Pulverized coal flames, Ph.D Thesis, University of London and the diphoma of membership of the imperial college, 1985

[13] Thailand Institute of Scientific and Technology Research (2015). *Characteristics of rubber wood pellet report 2015*.